Substrate Effect on the Crystallization of Isotactic Polypropylene

Yuan Lin, Yurun Fan

State Key Laboratory of Fluid Power Control and transmission, Zhejiang University, 310027 Hangzhou, China

Received 12 April 2011; accepted 18 August 2011
DOI 10.1002/app.35484
Published online 17 December 2011 in Wiley Online Library (wileyonlinelibrary.com).

ABSTRACT: The evolution of storage modulus measured by a rotational rheometer shows that the isothermal crystallization of isotactic polypropylene (iPP) melts in contact with aluminum plates (PP-Al) are considerably faster than that with stainless-steel plates (PP-SS). The difference is bigger at higher temperatures, and this behavior is opposite to that expected by our numerical simulation considering uniform bulk phase transition and substrate's ability to remove the latent heat. Polarized optical observations and surface energy evaluations via contact angle measurement indicate that surface energy of the substrates, including the effects of submicrometer morphology and roughness, should be the key factor to affect the crystallization of iPP. Transcrystallization zones, in which the nucleation density is controlled by the surface energy of substrates, were observed to grow toward the bulk with the thickness of about 0.2 mm for iPP to affect the global crystallization behavior. The critical value of surface energy of substrate to promote the interfacial crystallization of a polymer melt is derived, in terms of which the aluminum and stainless steel as well as optical glass, promote the surface nucleation with respect to the bulk nucleation of iPP. As a consequence, the conventional differential scanning calorimetry measurement mainly gives the heat fluxes of interfacial crystallization rather than the bulk crystallization due to the large surface-to-volume ratio of the specimen and the aluminum pan used which is a high surface energy substrate. © 2011 Wiley Periodicals, Inc. J Appl Polym Sci 125: 233–245, 2012

Key words: polypropylene; crystallization; interfaces

INTRODUCTION

In both experimental and industrial conditions, polymers are crystallizing in contact with substrates usually with large surface-to-volume ratio. Plastic products are often molded into hollow structures with thin walls using metal moulds; during the differential scanning calorimetry (DSC) measurement, aluminum pans are often used as the substrate[1–4]; while in the rheological experiments, a pair of plates of stainless steel with thickness of 1–2 mm is often used[5–9] to sandwich the polymer melt; and when using the hot stage microscopy, which has been applied successfully for determining the numbers of nuclei and measuring the growth rate of spherulites,[10–12] ultra thin polymer specimen is usually covered by glass plates. It is not surprising that, for an apparently same temperature history, the crystallization behavior and morphology in these experiments can be quite different; it is attributed to the large surface-to-volume ratio contact of polymers and substrates, including the effects of latent-heat-transfer ability, surface energy and roughness of the substrate, systematic errors, and the diversity of polymer samples used.[13–15]

Heat transfer plays an important role during polymer crystallization.[13,14] The liberation of latent heat of fusion will cause temperature increase in the specimen during an apparent "isothermal" crystallization due to the poor heat conduction ability of macromolecule materials, and the temperature increase will slow down the solidification in return. Thermal effects in iPP crystallization were carefully studied by Piorkowska[13] who calculated the temperature buildup at the crystallization front as well as that due to the crystallization of numerous spherulites in an iPP plate, by using the one-dimensional bulk heat generation function; she found that the temperature at the center is always higher than that at the border, and the temperature increase depends on the initial temperature and the sample's thickness. Her predictions were confirmed by experimental temperature measurements of the bulk crystallizing of iPP. However, the effect of substrate's heat transfer ability has not been taken into consideration in Piorkowska's study. Our previous work on the isothermal crystallization of HDPE on aluminum, brass, and stainless-steel plates indicated that the substrate's ability to remove the latent heat of crystallization should be taken into consideration.[15]

Correspondence to: Y. Fan (yurunfan@zju.edu.cn).
Contract grant sponsor: National Natural Science Foundation of China; contract grant number: 10472105.

Surface-induced crystallization of polymers has attracted considerable attention during the past decades; see the excellent review by Li and Yan.[16] It is well documented that a foreign surface can alter the crystallization kinetics as well as the resultant crystal structure and morphology of a polymer via the interfacial arrangement of crystallographic orientations, the so-called epitaxy mechanism. A well-known phenomenon of the surface-induced crystallizations is the so-called transcrystallization, which is caused by the heterogeneous nucleation at the interface between polymer melts and substrates.[17–24] The prerequisite for transcrystallization growth is the presence of high density of active nuclei on the substrate's surface; the crowding of nucleus hinders the lateral growth of spherulites, and, consequently, the crystalline phase can develop only in perpendicular to the interface forming a crystalline front parallel to the interface and developing further into the bulk until meeting the spherulites formed in the bulk melt. Billon et al.[20] performed nonisothermal crystallizations of HDPE with various thickness and cooling rates and found that the presence of transcrystallization could greatly influence the DSC measurements. Yuryev et al.[25] carried out detailed investigation on the isothermal surface/bulk crystallizations of poly(L/D-lactide) by using DSC measurements as well as the Monte-Carlo simulations and showed that the surface crystallization dramatically affects the crystallization kinetics, changing both the crystallization rate and the very shape of crystallization curve; both the surface and bulk nucleation concentrations decrease when the crystallization temperature increases.

It has been found that surface nucleation rate, which controls the surface crystallization and the final transcrystallization zone, is largely determined by the substrate's surface energy (or the interfacial free energy difference).[18,21,22,25] However, most of the substrates used in previous studies are silicon based or fibers (glass, carbon, PET, and PTEF), the effect of surface energy on the intrfacial crystallization induced by metallic materials, which are prevalent in industrial applications as well as in rheological experiments has been rarely investigated.

In the present study, the isothermal crystallizations of an iPP (isotactic polypropylene) contacting with metallic plate made of aluminum and of stainless steel, respectively, are investigated by using rheological, optical, and surface-free-energy measurements. Two factors that cause the big difference in crystallization behavior of iPP are examined: the heat transfer and the surface properties of the substrates. Via numerical heat-transfer simulation, polarized microscopic observation on quenched specimens, and surface free energy measurement of the substrates, the effects of the two factors are assessed. A critical value of the substrate's surface free energy required to promote the surface nucleation with respect to the bulk nucleation of polymer melts is also derived. Finally, contribution of the surface crystallization to the global crystallization of iPP is analyzed using the data from optical, rheological, and DSC measurements.

EXPERIMENTAL

Materials

A commercial iPP (T300, Shanghai Petrochemical Corporation) was used in present study, which has the following characteristics: the molecular weights $M_n = 8.0 \times 10^4$ and $M_W = 3.3 \times 10^5$, and the melt flow rate (MFR) = 3.0 g/10 min.

Two kinds of metallic substrate in the form of round plate were used in the experiments, and they are made of aluminum and stainless steel, respectively, with the diameter of 25 mm and the thickness of 2 mm. Surfaces of the substrates were carefully polished by using SiC papers (grit 2500) to achieve approximately the same roughness. The morphology of the two manual smoothed metal plates was analyzed by using VH-Z500R Digital Microscope (Keyence) as shown in Figure 1(a,c). The roughness of substrates was measured by using Surfcorder SE3500 Surface Roughness Measuring Instrument (Kosaka Laboratory). Each of the plates was measured by four lines in different directions along the radius. The average roughness (R_a) of the aluminum and stainless steel plates are 0.045 ± 0.005 μm and 0.037 ± 0.01 μm, and the peak-to-valley roughness (R_z) are 0.22 ± 0.06 μm and 0.135 ± 0.06 μm, respectively. Typical roughness profiles measured are also shown in Figure 1(b,d). On the micrometer scale, the two kinds of plates have approximately the same roughness, but their apparent optical morphologies seem quite different.

Characterizing crystallization by rheological measurement

Rheological experiments were performed on a Gemini-200 rotational rheometer (Bohlin Instruments). Parallel plates made of the foregoing mentioned stainless steel and aluminum were used to sandwich the iPP specimen of 1 mm thickness. The combination was enclosed in a temperature control chamber of the rheometer and first heated and kept at 200°C for 10 min, and then the chamber was cooled at the rate of 40°C/min and then kept at a preset crystallization temperature. The temperature fluctuations were less than ±0.2°C in the later isothermal crystallization process. The temperature was measured by a thermal couple imbedded in the

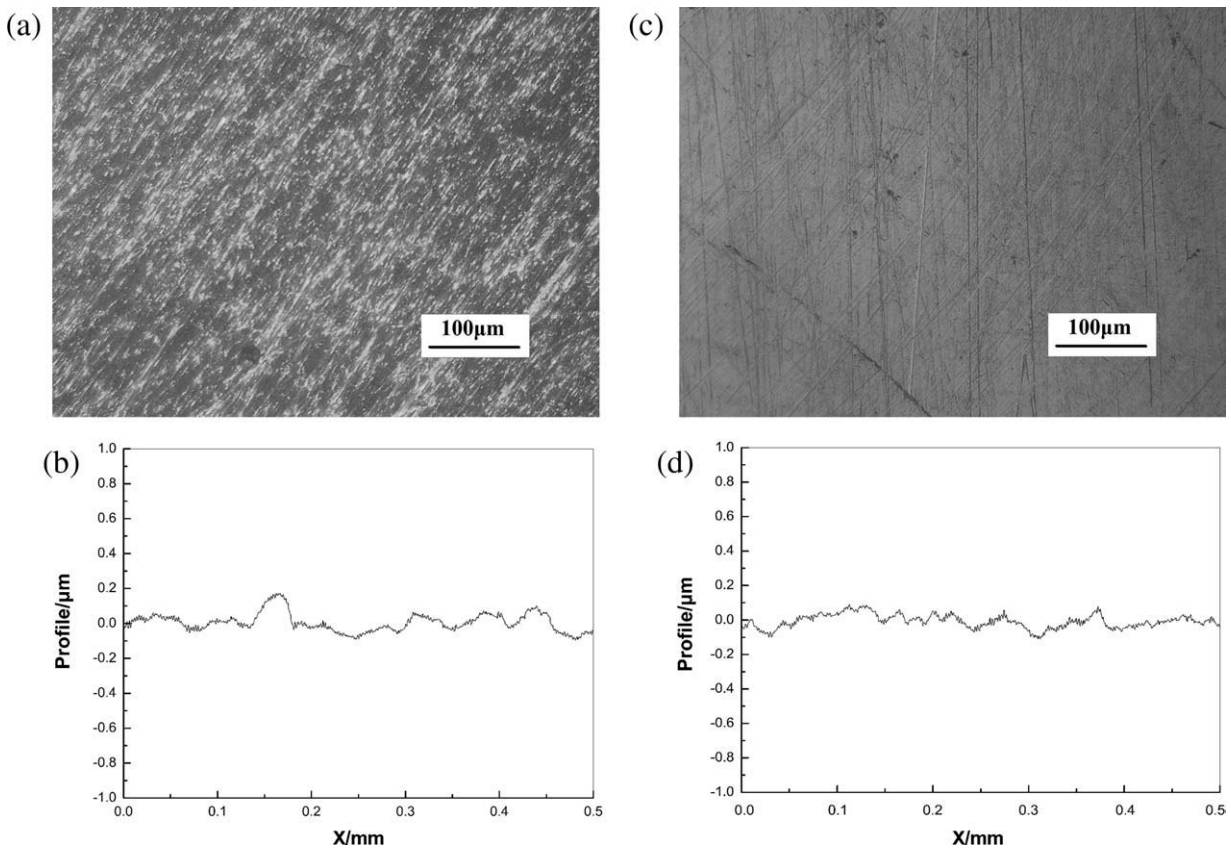

Figure 1 (a) Morphology of the surfaces of aluminum substrate; (b) profile of the surface of aluminum substrate; (c) morphology the surface of stainless steel substrate; (d) profile of the surface of stainless steel substrate.

center of the lower plate. During the isothermal crystallization, the small-amplitude oscillatory shearing with the strain of 0.5% and the angular frequency of 0.1 rad/s was carried out. It was confirmed that the strain used is small enough that the measured moduli are only time dependent and not strain dependent during the iPP crystallization, that is, the crystallization was not affected considerably by the small-strain oscillatory shearing. It is a common practice that the evolution of the storage modulus is used to characterize the crystallization process.[5–7]

Characterizing crystallization by DSC measurement

The DSC measurements were carried out by using the Perkin-Elmer DSC system 7. The iPP specimens were prepared in two different ways: in the accustomed way, the specimen was cut into small grains and placed in an aluminum pan for measurement; while in the special way, the iPP was melted and pressed to be a film with about 0.2 mm thickness beforehand, and a disk-shaped specimen was cut off from the film and introduced into the aluminum pan. The same temperature conditions as the rheological test were used in the DSC measurement: the cooling rate from 200°C to the crystallization temperature was set to 40°C/min.

Characterizing morphology by polarized microscopic observation

At the temperature of 200°C, small iPP grains were melted down between the foregoing mentioned metallic plates (aluminum or stainless steel), and the specimen was pressed to 10–20 μm thickness and kept at 200°C for 10 min to erase the deformation history. Afterward, the temperature was dropped down to the crystallization temperature at 40°C/min and kept constant for a preset time, and then the fixture-specimen was quenched by dropping it into cool water to frozen the iPP's morphology. The quenched iPP specimen (in 10–20-μm thick film) was observed on a polarizing microscope, and photos were taken to observe the nuclei or spherulites.

In addition, iPP disks with thickness of about 1 mm crystallized from the rheological measurements were sliced up along the thickness direction, and the slices of about 8 μm thickness were observed using the polarizing microscope to analyze the morphology in the thickness direction.

Measurement of surface energy of substrates

Using the method proposed by Hallab et al.,[26] the total surface energy and its dispersive and polar components for the aluminum and stainless steel plates were determined by measuring the contact angles with four liquids of known surface tensions: water, ethanol, benzene, and ethylene glycol. A series of eight liquid drops were placed on the horizontal aluminum or stainless-steel plate, and the contact angles θ were measured using Cam 200 Optical Contact Angle Meter (KSV, Finland), and the mean value of the eight drops was calculated. To determine the polar and dispersive components of surface energy of the substrate, the Young's equation is used,

$$\cos\theta = \frac{\gamma_{SV} - \gamma_{SL}}{\gamma_{LV}} \tag{1}$$

where γ_{SV}, γ_{SL}, and γ_{LV} denote the solid/vapor, solid/liquid, and liquid/vapor interfacial energy, respectively. The interfacial energy between phase a and phase b can be expressed by using the surface energy (surface tension) of each phase:

$$\gamma_{ab} = \gamma_a + \gamma_b - 2\sqrt{\gamma_a^d \gamma_b^d} - 2\sqrt{\gamma_a^p \gamma_b^p} \tag{2}$$

where the upper-index d and p denote the dispersive and polar component, respectively. Applying eq. (2) to eq. (1) yields

$$1 + \cos\theta = \frac{2\sqrt{\gamma_S^d \gamma_L^d}}{\gamma_L} + \frac{2\sqrt{\gamma_S^p \gamma_L^p}}{\gamma_L} - \frac{\pi_e}{\gamma_L} \tag{3}$$

where $\pi_e = \gamma_S - \gamma_{SV}$ is the spreading pressure. As proposed by Schakenraad et al.,[27] a linear approximation between the spreading pressure and the surface tension can be assumed for various liquids: $\pi_e = A\gamma_L + B$, where A and B are empirical constants. Performing contact angle measurements of the four liquids with known surface tensions γ_L^d, γ_L^p enables us to determine the constants A and B and the surface energies γ_S^d and γ_S^p by using eq. (3).

NUMERICAL SIMULATION OF HEAT TRANSFER IN "ISOTHERMAL" CRYSTALLIZATION

The finite volume method in the FLUNT software is adopted to solve the unsteady heat transfer problem of the "isothermal" crystallization process of an iPP specimen sandwiched between two metallic plates. The governing equation is

$$\frac{\partial T}{\partial t} = \alpha\nabla^2 T + \frac{q}{\rho c_p} \tag{4}$$

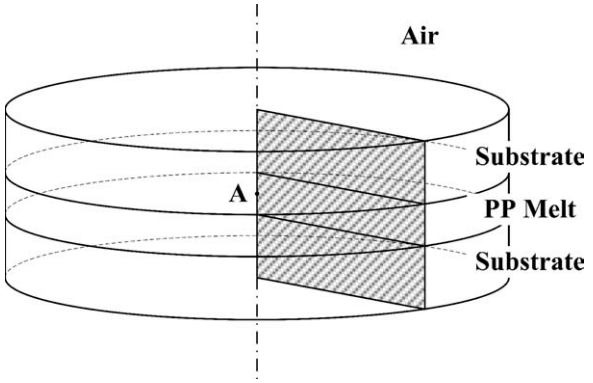

Figure 2 Diagram for numerical simulation of heat conduction during 'isothermal' crystallization in the rheology experiment.

where ρ, c_p are density and heat capacity, respectively, and $\alpha = k/\rho c_p$ is the heat diffusivity, where k is the heat conduction coefficient, and q denotes the time-dependent heat source due to the latent heat release of crystallization. The configuration, diagramed in Figure 2, and the boundary conditions are the same as the rheological experiment, that is, an iPP specimen of 1 mm thickness and 25 mm diameter sandwiched by two plates made of aluminum or stainless steel with the thickness of 2 mm and diameter of 25 mm. The temperature at the outer surfaces of the sandwich system (including the outer metal surfaces and the surface of iPP specimen exposed to air in the oven of rheometer) is assigned. According to the rheological experiment, the simulation includes the cooling period in which the outer temperature drops from 200°C at 40°C/min to a constant crystallization temperature as well as the subsequent "isothermal" crystallization period. It is assumed that the crystallization does not take place during the temperature-dropping period, and the small temperature fluctuations taking placing in the rheological experiments after the system reached to the target crystallization temperature is neglected in the simulation. Because the problem is axi-symmetric, the computation can be carried out on a rectangular domain as the shaded area in Figure 2.

The conductivity, density, and heat capacity of the crystal and melt phases of iPP specimen are assumed to be the same, their values, taken from the reference,[13] are listed in Table I, together with the thermal parameters of aluminum and stainless-steel plates, which were measured and reported in our previous research.[15]

The most difficult part of simulation is to estimate the time-dependant latent heat source q in eq. (4), that is, we need *a priori* the kinetics of nucleation and spherulite growth of iPP. As a plausible procedure, we adopt the kinetics reported in the literature for the bulk crystallization of iPP and neglect the

TABLE I
Thermal Parameters of the iPP, Aluminum, and Stainless Steel Plates Used in the Numerical Simulation

Parameters	Al	Stainless steel	iPP
c_p [J/(kg K)]	970	510	2095
ρ (kg/m^3)	2761	7886	854
k [W/(m K)]	141.68	15.05	0.17
α [(10^{-5} m^2/s)]	5.296	0.373	0.0095

substrate's effect. Also, we assume the athermal nucleation mechanism, that is, the simultaneous appearance of nuclei at the beginning of the crystallization temperature. Piorkowska[13] proposed the following equation for the temperature dependence of the number of nucleus per unit volume based on experimental data:

$$D = C_1 \exp(-C_2 T) \tag{5}$$

where D is the number of nucleus per cubic meter. We fitted the experimental data on the number of nucleus of iPP collected by Janeschitz-Kriegl et al.[29] and obtained $C_1 = 2.23 \times 10^{19}$/m^3 and $C_2 = 0.1567$ K^{-1}. The temperature dependence of spherulite growth rate of iPP takes the form:

$$G(T) = G_0 \exp\{-U[R(T - T_\infty)]^{-1}\} \times \exp\left\{-K_g[T(T_m^0 - T)]^{-1}\right\} \tag{6}$$

where the values of $G_0 = 8009$ cm/s, $U = 1500$ cal/mol, $K_g = 358400$ K^2, $T_\infty = 231.2$ K, the equilibrium melting point $T_m^0 = 458.2$K were reported in the Ref. 13. Given the above kinetics of iPP crystallization, the evolution of relative crystallinity with time can be calculated by the Kolmogoroff equation[30]

$$\alpha(t) = 1 - \exp\left\{-\frac{4}{3}\pi D\left[\int_0^t G(z)dz\right]^3\right\} \tag{7}$$

The instant rate of latent heat liberation is estimated to be $q = (\Delta H)d\alpha/dt$, where ΔH is the total latent heat released during the isothermal crystallization; $\Delta H \approx 109 \times 10^6$ J/m^3 at 130°C and $\Delta H \approx 104 \times 10^6$ J/m^3 at 127°C obtained by our DSC measurement (in Ref. 13 $\Delta H \approx 119 \times 10^6$ J/m^3 at 130°C).

In an apparent "isothermal" crystallization process, the temperature field evolves with the time due to the latent heat release and conduction. To be specific, the temperature variation at the center of iPP sample, that is, the point A in Figure 2, with respect to the environmental (outer surface) temperature during the crystallization, is traced to represent the nonuniformity of the temperature field.

RESULTS AND DISCUSSION

By rheological measurement, the evolution of the storage modulus with the time can be used to characterize the global crystallization rate of various polymer materials (see, e.g., Refs. 5–7). Figure 3 shows the great influence of the fixture-plates on the crystallization of iPP specimen: the crystallization of iPP melts in contact with the aluminum plates (PP-Al) is faster than that with the stainless-steel plates (PP-SS), and, furthermore, the difference of crystallization rate becomes larger at higher crystallization temperature. Similar phenomenon has been mentioned by Menzel et al.,[31] who discovered that in DSC measurements the pan's material (aluminum, gold, and platinum) has strong effect on the crystallization of iPP, but no systematic pursuit on the

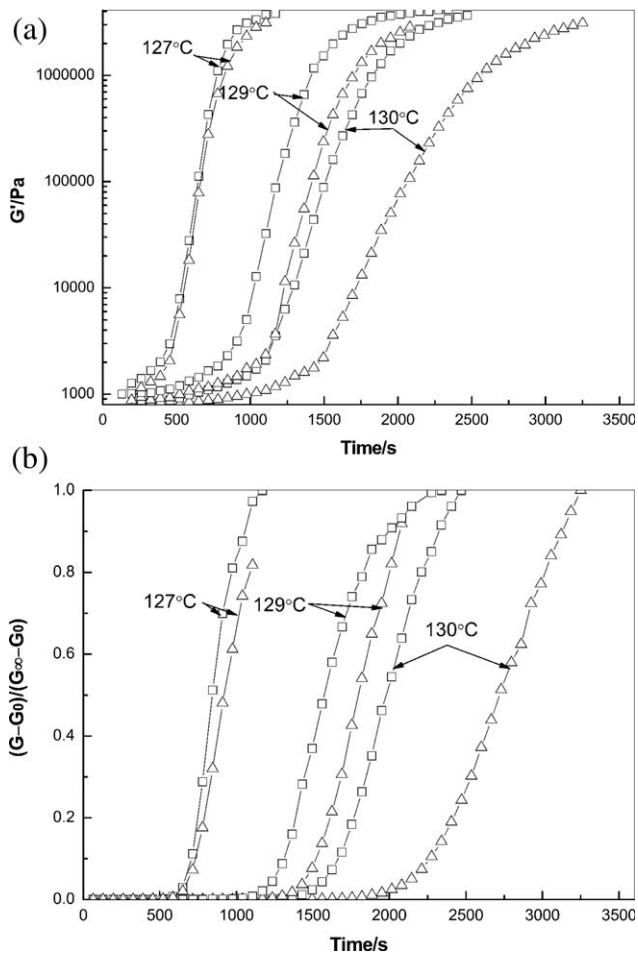

Figure 3 (a) Evolutions of absolute storage modulus of the iPP melt crystallizing at 127, 129, and 130°C in the small amplitude oscillation shearing measurements by the parallel plates made of aluminum (squares) and made of stainless steel (triangles). The iPP specimen's thickness is 1.0 mm. (b) Evolutions of relative storage modulus of the iPP melt crystallizing at 127, 129, and 130°C in the small amplitude oscillation shearing measurements by the parallel plates made of aluminum (squares) and made of stainless steel (triangles). The iPP specimen's thickness is 1.0 mm.

origin of this phenomenon was carried out in their work.

In our previous work on the crystallization of HDPE,[15] it was proposed that substrate's ability to remove the latent heat of crystallization is the key factor that affects the crystallization rate based on the observation that the isothermal crystallization rate decreases as the HDPE specimen contacts with aluminum, brass, and stainless-steel plates, respectively, which is in the same decreasing sequence of the thermal diffusivity of these metallic substrates. In this study, to study in depth the substrate's heat-conduction effect in "isothermal" crystallization processes, numerical heat transfer simulations for the crystallization of iPP between the aluminum plates (PP-Al) and stainless steel plates (PP-SS) were carried out based on the crystallization kinetics described in Numerical simulation of heat transfer in "isothermal" crystallization section, in which the environmental temperature drops from 200°C to 127°C or to 130°C and is kept constant thereafter; the results are shown in Figure 4. During the cooling process to the temperature of 130°C, shown in Figure 4(a), the temperature difference between the center of specimen and the outer surface of substrate is about 0.8 and 1.2°C for aluminum and stainless steel, respectively. As soon as the environmental temperature reaches the target value, the temperature differences drop quickly to less than 0.1°C for both the aluminum and stainless-steel plates. The cooling period lasts less than 110 s, which is rather a short time compared to the characteristic time of iPP crystallization at the target temperature. We assume that the influence on crystallization of the cooling period is negligible, and crystallization commences with the end of cooling period with the uniform temperature field. During the "isothermal" crystallization period, shown in Figure 4(b), it is reasonable to assume that the maximum temperature difference between the center of iPP layer and the outer surface of metallic substrates roughly represent the maximum instant crystallization rate, and the solidification is finished when the temperature difference again approaches to zero. It is noticed that although the coefficient of heat diffusion of aluminum is one order of magnitude larger than that of stainless steel (see Table I), there are no noticeable differences between the times when PP-Al and PP-SS reach the maximum crystallization rate as well as that when the solidification is finished. Actually, the thermal resistances (α^{-1}) of the two metallic substrates are too small compared to that of iPP for their difference to significantly affect the crystallization behavior of iPP. In Figure 4(b), the temperature curves of PP-Al and PP-SS tend to superpose each other when the crystallization proceeds at the higher temperature. This behavior should be expected, because, at higher

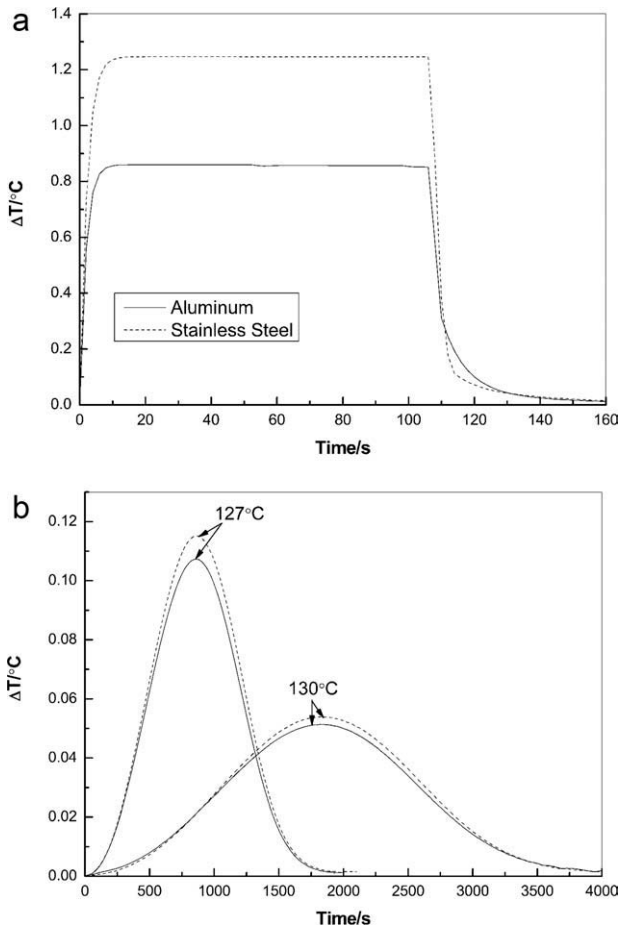

Figure 4 (a) Evolutions of the temperature difference between the center of iPP specimen and the outer surface of metal substrates by the numerical simulation of cooling period when the measured temperature is dropped from 200 to 130°C with the aluminum (real line) and stainless steel (dashed line) plates. (b) Evolutions of the temperature difference between the center of iPP specimen and the outer surface of metal substrates by the numerical simulation of isothermal crystallization period of iPP with the aluminum (real line) and stainless steel (dashed line) plates, at the temperature of 127 and 130°C, respectively.

temperatures, the crystallization slows down, so does the rate of latent heat release, leading to smaller temperature differences between the center of iPP layer and the environment. However, the rheological measurement shown in Figure 3 indicates that the difference of crystallization rates of iPP sandwiched by the aluminum plates and by the stainless-steel plates gets larger at higher temperatures, which is an opposite behavior to the effect of heat transfer. Therefore, the ability to remove the latent heat produced by crystallizing iPP seems not a key factor responsible for the large differences of crystallization behavior on the metallic substrates, other properties of the substrates must be taken into consideration.

It is well known that surface energy of substrate has large impact on the surface crystallization of

polymer materials.[18,21,22] Let us first examine the effect of surface energy of substrate on the nucleation rate of polymers. Nucleation rate in polymer melts can be expressed by

$$I = I_0 \exp[-(\Delta G^* + \Delta G_\eta)/kT] \quad (8)$$

where I_0 is a rate constant, ΔG_η is the activation energy for molecules to cross the phase boundary, k is the Boltzmann's constant, T the crystallization temperature, and ΔG*is the critical free energy barrier for creating a nucleus, which is the maximum value of Gibbs free energy ΔG with respect to the nucleus' geometrical dimensions a, b, and l. According to Wunderlich,[32] the Gibbs free energy can be expressed as

$$\Delta G(a,b,l) = -abl\Delta g_f + 2al\gamma_{cm} + 2bl\gamma_{cm} + 2ab\gamma_e \quad (9)$$

for the case of homogeneous nucleation, which we assume to be the mechanism for bulk nucleation and

$$\Delta G(a,b,l) = -abl\Delta g_f + al\Delta\gamma + 2bl\gamma_{cm} + 2ab\gamma_e \quad (10)$$

for the case of heterogeneous nucleation, which is appropriate for the nucleation with the presence of foreign surfaces, where γ_{cm}, γ_e are the lateral-side/melt and the fold-end/melt interfacial energy, respectively; Δg_f is the bulk free energy of nucleus per unit volume; $\Delta\gamma$ is the interfacial free energy difference and can be expressed by (see Cherry[33])

$$\Delta\gamma = \gamma_{cm} + \gamma_{cs} - \gamma_{ms} \quad (11)$$

where γ_{cs} is the crystal/substrate interfacial free energy and γ_{ms} is the melt/substrate interfacial free energy. Applying eq. (2) to eq. (11), $\Delta\gamma$ can be further expressed as

$$\Delta\gamma = \gamma_{cm} + \gamma_c - \gamma_m + 2\sqrt{\gamma_m^d\gamma_s^d} - 2\sqrt{\gamma_c^d\gamma_s^d} + 2\sqrt{\gamma_m^p\gamma_s^p} - 2\sqrt{\gamma_c^p\gamma_s^p} \quad (12)$$

Since the polar components of iPP are negligibly small compared to the dispersion component,[18] eq. (12) is simplified to

$$\Delta\gamma \approx \gamma_{cm} + \gamma_c^d - \gamma_m^d - 2\sqrt{\gamma_s^d}\left(\sqrt{\gamma_c^d} - \sqrt{\gamma_m^d}\right) \quad (13)$$

Notice that, using eq. (2), γ_{cm} can be expressed as

$$\gamma_{cm} = \gamma_c + \gamma_m - 2\sqrt{\gamma_c^d\gamma_m^d} - 2\sqrt{\gamma_c^p\gamma_m^p} \approx \gamma_c^d + \gamma_m^d - 2\sqrt{\gamma_c^d\gamma_m^d} \quad (14)$$

TABLE II
Values of Total, Polar, and Dispersion Surface Energy Components of Four Testing Liquids, Taken from Refs. 26 and 28

Liquid	γ^d (mJ/m^2)	γ^p (mJ/m^2)	γ (mJ/m^2)
Water	21.80	51.00	72.80
Ethanol	18.80	3.6	22.40
Ethylene glycol	29.00	19.00	48.00
Benzene	28.85	0	28.85

Maximizing ΔG with respect to a, b, and l for the case of heterogeneous nucleation (eq. 10) and using $\Delta g_f = \Delta T\Delta h_f/T_m{}^0$, the critical free energy barrier ΔG* is deduced to be

$$\Delta G^* = \frac{16\gamma_{cm}\gamma_e\Delta\gamma T_m^{0^2}}{\Delta T^2\Delta h_f^2} \quad (15)$$

where Δh_f is the heat of fusion per unit volume, T_m^0 is the equilibrium melting temperature, ΔT is the degree of supercooling. Equations (8) and (15) indicate that lower $\Delta\gamma$ corresponds to a lower energy barrier, thus higher nucleation rate. Equation (13) indicates that given γ_{cm}, γ_c^d, and γ_m^d, $\Delta\gamma$ is smaller with larger γ_S^d, that is, a substrate with high surface energy promotes the interfacial nucleation. If the surface energy is high enough, causing negative $\Delta\gamma$ (negative ΔG*), the energy barrier ΔG*becomes a promoter for the nucleation. Furthermore, in the case of $\Delta\gamma = 2\gamma_{cm}$, eq. (10) is equivalent to eq. (9), that is, the nucleation rate at the interface is equal to the bulk nucleation rate. By setting $\Delta\gamma = 2\gamma_{cm}$ in eq. (13) and inserting eq. (14), a critical surface-free energy of the substrate is obtained.

$$\gamma_s^{d*} = \gamma_m^d \quad (16)$$

That is, critical surface free energy of the substrate is equal to the surface energy of the polymer melt. In the case of $\gamma_s < \gamma_s^{d*}$, the nucleus density at the interface would not be increased by the presence of interface; in the case of $\gamma_s > \gamma_s^{d*}$, the nucleus density at the interface would be higher than the bulk density.

Roe[34] has reported the measured surface energy $\gamma_m(\approx\gamma_m^d)$ of iPP, which decreases linearly from 23.78 to 19.85 mJ/m^2 in the temperature range from 120 to 190°C. In this study, surface energies of the aluminum and stainless-steel plates were obtained by contact angle measurements of four testing liquids. The dispersion and polar components of surface energy of the testing liquids are listed in Table II, taken from the literature.[26,28] The mean contact angles for each liquid on each substrate and the surface energies of the substrates calculated by using eq. (3) are listed in Table III. It is seen that the aluminum

TABLE III
Average Contact Angle of the Test Liquids on Aluminum and Stainless-Steel Substrates and the Surface Energies of the Substrates

Substrate	Water	Ethanol	Benzene	Ethylene glycol	γ^d (mJ/m^2)	γ^p (mJ/m^2)
Aluminum	98.98	30.55	11.56	66.33°	82.05	0.98
Stainless steel	90.28	20.45	15.07	65.52°	31.37	0.88

(actually, aluminum oxide) has much higher surface energy than the stainless steel, but both the surface energies are higher than the critical one, $\gamma_s^{d*} \approx 20\text{mJ/m}^2$. As a consequence, the interfacial nucleation of iPP in contact with the aluminum or stainless-steel plates is promoted with respect to the bulk nucleation, and it is much easier for iPP to nucleate at the aluminum surface than at the stainless-steel surface.

By using a polarizing microscope, optical observations on the iPP slices with about 15 μm thickness crystallized at 130°C and sandwiched by the aluminum plates or by the stainless-steel plates are displayed in Figure 5, which shows the morphology of surface crystallization. Because of the small thickness, transcrystallization layer cannot be fully developed in these experiments, and so the morphology shown in Figure 5 is closely related to, but not the transcrystallization layers themselves that would develop in thicker specimen. The interfacial nucleation density of iPP slices can be estimated by counting the number of spherulites in Figure 5. Note that the numerous white tiny spots in these pictures are identified with the crystals formed during the later quenching process, because these white tiny spots were also observed when the iPP melt was directly quenched into cold water from the temperature of 200°C. So, they were excluded in the nucleus counting procedure. In fact, they are small spherulites formed during the fast cooling period of the final quenching (see Ref. 10). The growth rate of spherulites can also be estimated from Figure 5, which is about 7.8×10^{-8}m/s according to the photos of PP-SS. The growth rate of PP-Al is difficult to estimate due to the high number density and the earlier spherulite impingement.

To confirm the key effect of substrate's surface energy, the spherulite morphology of an iPP slice of about 15 μm thickness crystallizing between microscopic glass slides at 130°C is shown in Figure 6. The surface energy of the optical glass slide was measured by the procedure described in Experimental section in which the testing liquid of ethanol was replaced by glycerol. The dispersion component of surface energy of the glass slide lies between those of the stainless-steel plate and the aluminum plate. Table IV lists the number densities of spherulites counted at the crystallization temperature of 130°C and the surface energies of the three substrates, the number density increases as the surface energy of substrate increases, consistent with the above analyses. One can observe that the size of spherulites crystallizing on the glass slide is smaller than that crystallizing on the stainless steel plate but considerably larger than that crystallizing on the aluminum plate.

Morphology of the substrates' surface should also be considered. On the micrometer scale, the aluminum and stainless-steel plates have approximately the same roughness in terms of the average roughness (R_a) and the peak-to-valley roughness (R_z; see Experimental section). Considering the fluctuations in roughness measurement, there is an overlap range of roughness of the two metallic plates. However, as shown in Figure 1, the optical patterns seem quite different for the two plates. The big difference is possibly due to different morphologies on the length scale smaller than micrometer that may affect crystallization.[35] Compared to the metallic plates, the roughness of the glass plate is very small with $R_a < 0.01$ μm and $R_z < 0.09$. It is well known that surface roughness may considerably affect surface energy measurement. At the present stage, we consider that our measured surface energies of the aluminum, stainless steel, and glass plates have already included the influence of morphology on the length scales smaller than micrometer as well as the effect on the interfacial crystallization of iPP.

In the rheological experiments with the iPP thickness of about 1 mm, surface crystallization, in the form of transcrystallization, grew into the bulk to affect the global solidification. Typical morphology of transcrystallization due to heterogeneous nucleation at the interface of the iPP specimen and the substrates is shown in Figures 7 and 8, which are the cross section photos along the thickness direction of iPP disks. Figure 7 shows morphologies of the PP-Al samples crystallized in the small-strain oscillation shearing tests (a) and crystallized in quiescent state (b). No significant difference in the transcrystallization zones or in the bulk is noticed, indicating that the small strain (0.5%) in the rheological tests had little influence on the crystallization of iPP. β-Crystals of iPP [indicated by the white arrows in Fig. 7(b)] were formed occasionally in both dynamic and quiescent crystallization experiments, which might originate from the vacuum bubbles caused by the volume contraction in the later stage of

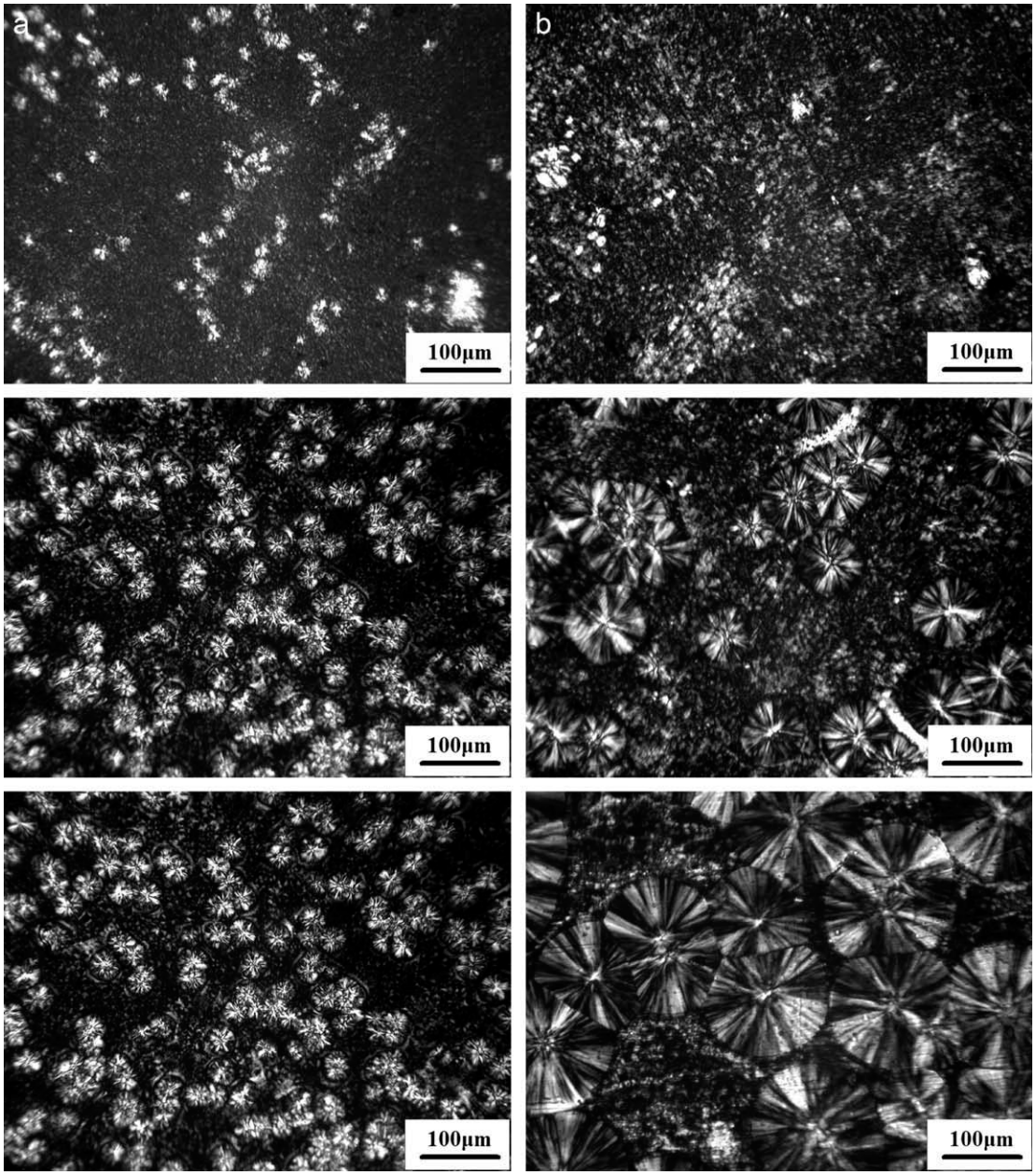

Figure 5 (a) (1) Optical observations on the quenched iPP specimen with ~ 15 μm thickness isothermally crystallizing at 130°C, on the aluminum substrate after the crystallization time of 3 min. (a) (2) Optical observations on the quenched iPP specimen with ~ 15 μm thickness isothermally crystallizing at 130°C, on the aluminum substrate after the crystallization time of 6min. (a) (3) Optical observations on the quenched iPP specimen with ~ 15 μm thickness isothermally crystallizing at 130°C, on the aluminum substrate after the crystallization time of 10 min. (b) (1) Optical observations on the quenched iPP specimen with ~ 15 μm thickness isothermally crystallizing at 130°C, on the stainless-steel substrate after the crystallization time of 3min. (b) (2) Optical observations on the quenched iPP specimen with ~ 15 μm thickness isothermally crystallizing at 130°C, on the stainless-steel substrate after the crystallization time of 7 min. (b) (3) Optical observations on the quenched iPP specimen with ~ 15 μm thickness isothermally crystallizing at 130°C, on the stainless-steel substrate after the crystallization time of 15 min.

crystallization.[36] Figure 8 shows cross sections of the iPP disks crystallized in stainless-steel plates and in glass slides (Note the crystallization in glass slides can only be carried out in static state, while PP-SS was crystallized under the small amplitude oscillation shearing.). From Figures 7 and 8(a), it is observed that the nucleation density of PP-SS at the interface seems to be lower than PP-Al, which is in consistence with the nucleation data from Figure 5. Varga et al.[24] reported that the unsized glass fibers did not induce transcrystallization in quiescent iPP melt. However, we observed the interfacial crystallization of iPP/glass-slides with the heterogeneous nucleation density higher than that in the bulk,

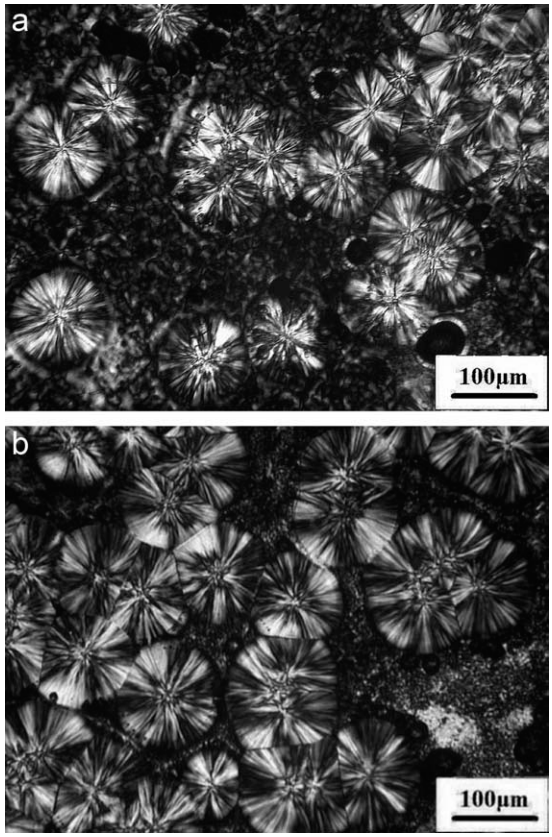

Figure 6 (a) Optical observations on the quenched iPP specimen with ~ 15 μm thickness isothermally crystallizing at 130°C on the optical glass plate after the crystallization time of 9 min. (b) Optical observations on the quenched iPP specimen with ~ 15 μm thickness isothermally crystallizing at 130°C on the optical glass plate after the crystallization time of 15 min.

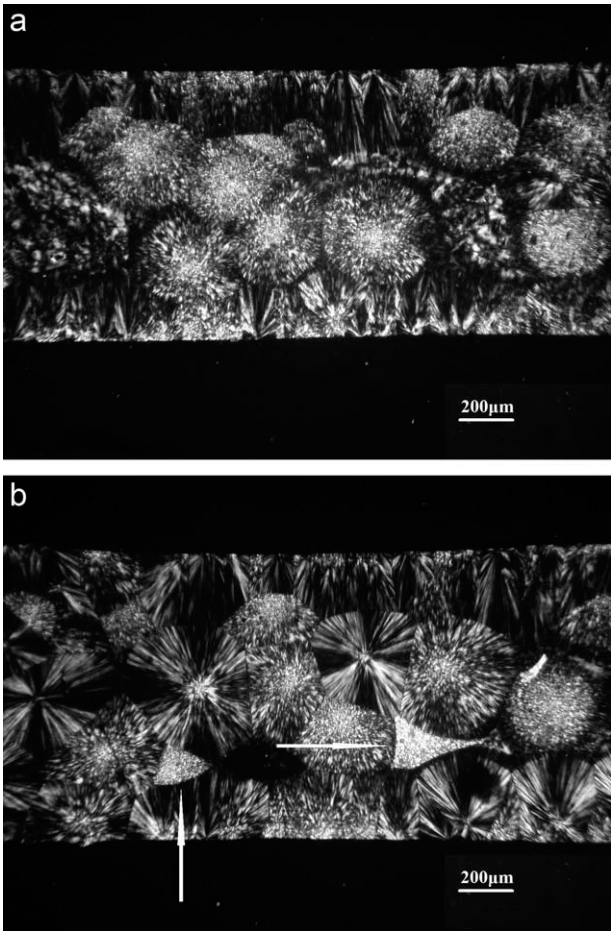

Figure 7 (a) Optical observations of the cross section of iPP plates isothermally crystallized at 130°C with aluminum substrates in rheological measurements with small amplitude oscillation. The iPP specimen's thickness is 0.1 mm. (b) Optical observations of the cross section of iPP plates isothermally crystallized at 130°C with aluminum substrates in static crystallization process. The iPP specimen's thickness is 1.0 mm.

especially at the lower side [see Fig 8(b)]. The enhancement of nucleation density by glass slides was also reported by Piorkowska et al.[37] However, Figure 8(b) does show that the transcrystalline zone had not been well developed on glass slides, it may be due to the very smooth surface of glass slides. From Figures 7 and 8(a), the thickness of transcrystalline zones of PP-Al and PP-SS is estimated to be about 200 μm. The presence of aluminum or stainless-steel surface accelerated the crystallization of iPP with respect to the bulk crystallization and the interfacial crystallization of PP-Al was faster than that of PP-SS. This explains the global variation of crystallization rates observed in the rheological experiment (Fig. 3).

TABLE IV
Surface Energies of Aluminum, Stainless Steel, Glass Plates, and the Corresponding Nucleation Densities of iPP Slices

	Aluminum	Glass	Stainless steel
γ^d (mJ/m^2)	82.05	39.45	31.37
Nucleus density (m^{-2})	5.81×10^8	1.2×10^8	9.0×10^7

Let us apply the Piorkowska's model for the crystallization kinetics of iPP, expressed by eqs. (5)–(7), to the transcrystallization region of about 200 μm thickness. As suggested by Janeschitz-Kriegl,[29] the number of spherulites per unit area counted on a thin slice can be raised by the power 3/2 to obtain a reliable approximate value for the number of spherulites per unit volume. To fit the nucleation and growth data of our thin slice experiments at 130°C, the constant C_1 in eq. (5) was modified to 9.84×10^{21}/m^3 for PP-Al and 6.0×10^{20}/m^3 for PP-SS, and the constant C_2 was unchanged, in eq. (6) $G_0 = 62.82$m/s was used for both PP-Al and PP-SS. The evolutions of relative crystallinity of the iPP specimen contacting with aluminum plates and contacting with stainless-steel plates, at the temperatures of 130 and 127°C, were calculated by using eq. (7), and

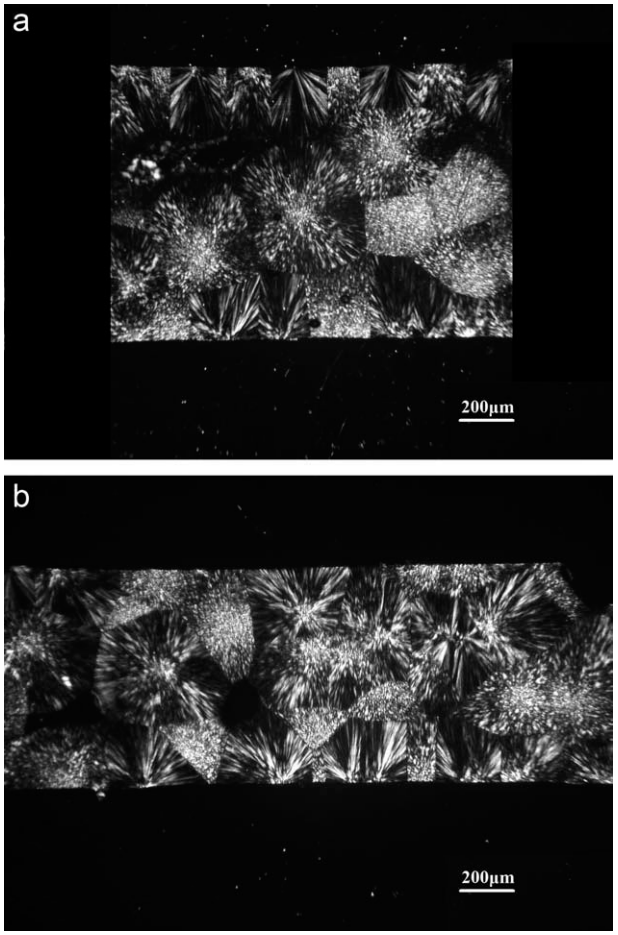

Figure 8 Optical observations of the cross section of iPP plates isothermally crystallized at 130°C in contact with stainless steel substrates. The iPP specimen's thickness is 1.0 mm. (b) Optical observations of the cross section of iPP plates isothermally crystallized at 130°C in contact with glass slides. The iPP specimen's thickness is about 1.0 mm.

the results are shown in Figure 9. Note that in the calculation, the latent heat was neglected considering the very thin slices of iPP specimen. Also noted is that the characteristic crystallization times in Figure 9 are much shorter than that of the rheological experiments shown in Figure 3, because the crystallization rate in the thin slices is dominantly affected by the substrates, while in the rheological experiments, the specimen is much thicker ($\sim$ 1 mm), and the bulk crystallization has lower nucleation density. However, Figure 9 shows the same qualitative behavior as in the rheological experiments (Fig. 3): the difference of the crystallization rate contacting with the aluminum plate and with the stainless-steel plate gets bigger at the higher temperature.

Rheological measurements on the iPP specimen of 200 μm thickness were carried out, in which the surface crystallization should dominate the process, and the results are shown in Figure 10. It can bee seen

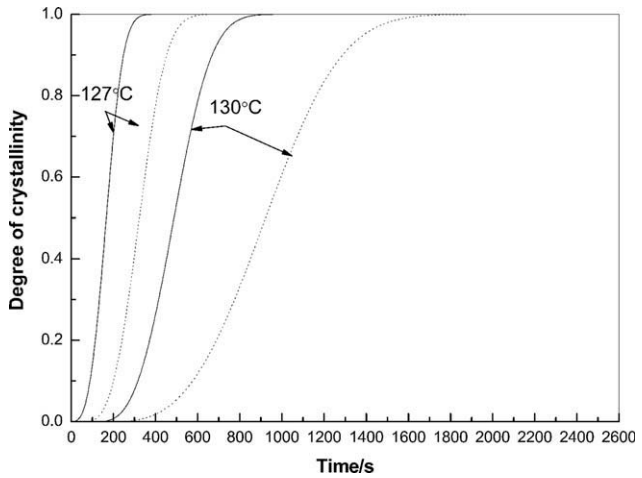

Figure 9 Evolutions of the relative crystallinity of iPP crystallizing at 127 and 130°C, in contact with aluminum (solid line) and stainless steel (dashed line) plates, obtained by using the Piorkowska's model with eqs. (5)–(7) in which the nucleation constants are modified according to our optical measurement.

that by reducing the thickness of iPP specimen, the time scale of rheological measurement shortens and approaches to the time scale of Figure 9 obtained by the simulations based on surface nucleus counting. The accordance between the results of optical and rheological experiments indicates that the surface energy of substrate indeed plays a key role in the interfacial nucleation and consequently influences the global crystallization rate and morphology of thick samples.

We implemented DSC measurements on the iPP crystallization by using two kinds of specimen: in the accustomed form of tiny grain and in the special form of thin film, the results are shown in Figure 11.

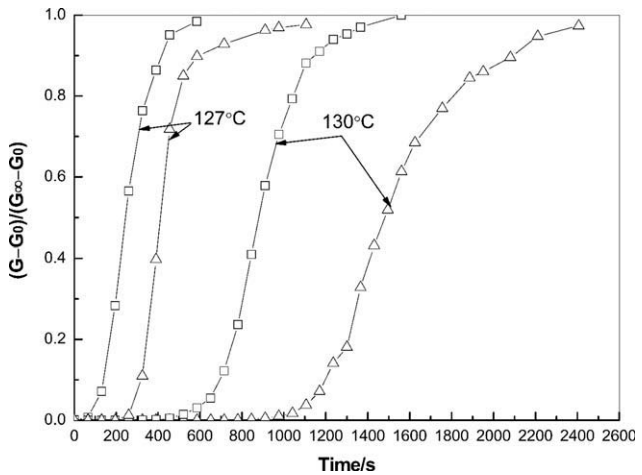

Figure 10 Evolutions of the relative storage modulus of the iPP melt crystallizing at 127 and 130°C in the small amplitude oscillation shearing measurements by the parallel plates made of aluminum (squares) and made of stainless steel (triangles). The iPP specimen's thickness is 0.2 mm.

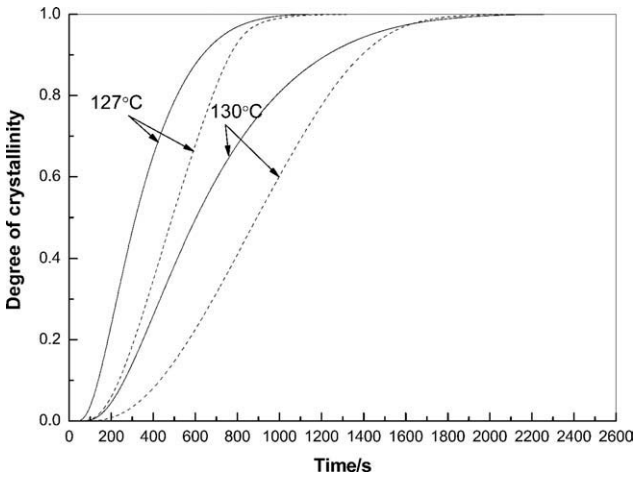

Figure 11 Evolutions of the relative crystallinity obtained by DSC measurements of the iPP specimens prepared in tiny grain (solid line) and prepared in thin film (dashed line) crystallizing at 127 and 130°C, respectively.

The samples after DSC measurement were both in disk shape, with the thickness of 0.3–0.4 mm for the accustomed way and 0.2–0.3 mm for the special way. The iPP specimen prepared in the grain form crystallized faster than that prepared in the film form. The small grain of iPP melted and formed a porous disk during the thermal preservation period at the temperature of 200°C before the isothermal crystallization; the porosity may be favorable to surface crystallization by increasing the contact area. The characteristic crystallization time, defined as the time when the relative storage modulus in rheological measurement or the degree of crystallinity in DSC measurement reaches to 0.5, is adopt to represent the overall crystallization rate. The values of characteristic crystallization time estimated from Figures 3, 10, and 11 are listed in Table V. Both the characteristic crystallization times in the DSC measurement with the specimen prepared in two ways are somewhat near that in the rheological measurement where the specimen of 0.2 mm thickness sandwiched between aluminum plates, but are considerably smaller than that where the specimen of 1.0 mm thickness sandwiched between aluminum plates. This implies that the conventional DSC measurement mainly gives the heat flux of the interfacial crystallization rather than the bulk crystallization, because during the measurement specimen has a large surface-to-volume ratio and contacts with an aluminum pan, which is a substrate of high surface energy.

CONCLUSIONS

The evolution of storage modulus measured by a rotational rheometer has shown that the crystallization of iPP melts in contact with substrate made of aluminum is considerably faster than that in contact with substrate made of stainless steel. The numerical simulation for the heat transfer problem of the apparent isothermal crystallization shows that the substrate's ability to remove the latent heat is a rather weak factor. Moreover, the difference of crystallization rate in rheological experiment becomes even greater at higher crystallization temperatures, this behavior is opposite to that expected considering the latent heat releasing in bulk phase transition as well as to that demonstrated by the heat conduction simulation.

Optical observation by using a polarizing microscope on the iPP slices of about 15 μm thickness crystallizing between the aluminum, glass, and stainless-steel plates, respectively, shows remarkable difference in the nucleation density and the size of spherulites. Via contact angle measurements, surface energies of the aluminum, glass, and stainless-steel plates were determined. A positive correlation between the surface nucleation density and the substrate's surface energy is revealed. A critical surface energy of substrate that will promote interfacial crystallization with respect to the bulk crystallization is deduced to be equal to the surface tension of the melt, in terms of which the aluminum, glass, and stainless-steel plates all promote the interfacial crystallization with respect to the bulk crystallization. On micrometer scale, the aluminum and stainless-steel plates have approximately the same roughness, but their morphologies on submicrometer scales seem quite different, and the glass plate is much smoother than the metallic plates. At the present stage, we consider that the measured surface energies have already included the influence of morphology on submicrometer scales.

The surface energies of substrates affect the global crystallization via the transcrystallization zone in which nuclei of higher number density than the bulk grow toward the bulk forming the thickness of about 0.2 mm in iPP specimen. Thus, the presence of aluminum or stainless steel surface accelerates the crystallization with respect to ideal bulk crystallization, and this explains the observed large difference in global crystallization behavior of iPP specimen in the form of 1-mm thick disk between the aluminum

TABLE V
Characteristic Crystallization Times from DSC and Rheological Measurements

Experiments		Rheology (mm)		DSC	
Sample thickness/form		1	0.2	Tiny grain	Thin film
Characteristic crystallization time (s)	127°C	840	250	307	490
	130°C	2010	900	597	894

plates and between the stainless-steel plates in rheological experiments.

The conventional DSC measurement mainly yields the heat flux of the interfacial crystallization rather than the bulk crystallization due to the large surface-to-volume ratio of the specimen and the aluminum pan used which is a high surface energy substrate. The interfacial crystallization (transcrystallization) has a great impact on characterizing the polymer crystallization by using rheologic or DSC measurements.

References

1. Schmidtke, J.; Strobl, G.; Thurn-Albrecht, T. Macromolecules 1997, 30, 5804.
2. Heck, B.; Hugel, T.; Iijima, M.; Sadiku, E.; Strobl, G. N J Phys 1999, 1, 17.1
3. Zhong, G. J.; Li, Z. M.; Li, L.; Shen, K. Polymer 2008, 49, 4271.
4. Shen, C. Y.; Zhou, Y. G.; Zheng, G. Q.; Liu, C. T.; Chen, J. B.; Li, Q. Polym Eng Sci 2008, 48, 2454.
5. Khanna, Y. P. Macromolecules 1993, 26, 3639.
6. Boutahar, K.; Carrot, C.; Guillet, J. J Appl Polym Sci 1996, 60, 103.
7. Boutahar, K.; Carrot, C.; Guillet, J. Macromolecules 1998, 31, 1921.
8. Chen, Q.; Fan, Y. R.; Zheng, Q. Rheol Acta 2006, 46, 305.
9. Wang, B.; Sun, G.; He, X.; Liu, J. Polym Eng Sci 2007, 47, 1610.
10. Eder, G.; Janeschitz-Kriegl, H. Mater Sci Technol 1997, 18, 269.
11. Janeschitz-Kriegl, H.; Eder, G.; Stadlbauer, M.; Ratajski. E. Monatshefte Chem 2005, 136, 1119.
12. Wang, J.; Qiang, D.; Wu, S.; Chen, X. Polym Eng Sci 2007, 47, 889.
13. Piorkowska, E. J Appl Polym Sci 1998, 66, 1015.
14. Janeschitz-Kriegl, H. Prog Colloid Polym Sci 1992, 87, 117.
15. Fan, Y. R.; Lin, Y.; Ruan, M. Z. J Cent South Univ Technol 2008, 15, 67.
16. Li, H. H.; Yan, S. Macromolecules 2011, 44, 417.
17. Binsbergen, F. L. Polymer 1970, 11, 253.
18. Cho, K.; Kim, D.; Yoon, S. Macromolecules 2003, 36, 7652.
19. Schonhorn, H. Macromolecules 1968, 1, 145.
20. Billon, N.; Henaff, V.; Pelous, E.; Haudin, J. M. J Appl Polym Sci 2002, 86, 725.
21. Wang, C.; Liu, C. R. Polymer 1999, 40, 289.
22. Wang, C.; Liu, F. H.; Huang, W. H. Polymer 2011, 52, 1326.
23. Quan, H.; Li, Z. M.; Yang, M. B.; Huang, R. Compos Sci Technol 2005, 65, 999.
24. Varga, J.; Karger-Kocsis, J. J Polym Sci Part B: Polym Phys 1996, 34, 657.
25. Yuryev, Y.; Wood-Adams, P. Polymer 2011, 52, 708.
26. Hallab, N. J.; Bundy, K. J.; O'Connor, K.; Moses, R. L.; Jacobs, J. J. Tissue Eng 2001, 7, 55.
27. Schakenraad, J. M.; Busscher, H. J.; Wildevuur, C. R. H.; Arends, J. J Biomed Mater Res 1986, 20, 773.
28. Zhao, Q.; Liu, Y.; Wang, C.; Wang, S.; Müller-Steinhagen, H. Chem Eng Sci 2005, 60, 4858.
29. Janeschitz-Kriegl, H.; Ratajski, E.; Wippel, H. Colloid Polym Sci 1999, 277, 217.
30. Kolmogoroff, A. N.; Izv Akad Nauk, S. S. S. R. Ser Math 1937, 1, 355.
31. Menczel, J.; Varga, J. J Therm Anal 1983, 28, 161.
32. Wunderlich, B. Macromolecular Physics; Academic Press: New York, 1976.
33. Cherry, B. W. Polymer Surfaces; Cambridge University Press: London, 1981.
34. Roe, R. J. J Phys Chem 1968, 72, 2013.
35. Alcazar, D.; Ruan, J.; Thierry, A.; Lotz, B. Macromolecules 2006, 39, 2832.
36. Varga, J.; Ehrenstein, G. W. Polymer 1996, 37, 5959.
37. Nowacki, R.; Monasse, B.; Piorkowska, E. Galeski, A.; Haudin, J. M. Polymer 2004, 45, 4877.